Clays and Clay Minerals, Vol. 61, No. 4, 290–302, 2013.

EVOLUTION OF DIOCTAHEDRAL VERMICULITE IN GEOLOGICAL ENVIRONMENTS – AN EXPERIMENTAL APPROACH

MICHAŁ SKIBA*

Institute of Geological Sciences, Jagiellonian University, ul. Oleandry 2a, 30-063 Kraków, Poland

Abstract—Dioctahedral vermiculite commonly occurs in soils and fresh sediments, but has not been reported in sedimentary rocks. Little is known of the evolution of this mineral during diagenesis. According to the available literature, dioctahedral vermiculite is likely to exhibit strong potential for selective sorption and fixation of K^+ involving interlayer dehydration and collapse. The objective of the present study was to investigate the influence of K^+ saturation and seawater treatments on the structure of dioctahedral vermiculite. Due to the fact that no dioctahedral vermiculite standard reference material was available, a natural sample of soil clay containing dioctahedral vermiculite was used in the study. The clay was saturated with K^+ using different protocols simulating natural processes taking place in soils and marine environments. The solid products of the experiments were analyzed for potassium content using flame photometry. The effect of the treatments used on the structure of dioctahedral vermiculite was studied using X-ray diffraction (XRD). The percentages of the collapsed interlayers were estimated by modeling the XRD patterns based on a whole-pattern multi-specimen modeling technique. All the treatments involving K^+ saturation caused K^+ fixation and irreversible collapse (*i.e.* contraction to 10 Å) of at least a portion of the hydrated (vermiculitic) interlayers. Air drying of the K^+-saturated samples greatly enhanced the degree of the collapse. The results obtained gave no clear answer as to whether time had had a significant effect on the degree to which irreversible collapse occurred. Selective sorption of K^+ from artificial seawater was observed. These results clearly indicate that collapse of dioctahedral vermiculite is likely to occur in soils during weathering and in sediments during early diagenesis. Both processes need to be taken into consideration in sedimentary basin studies.

Key Words—Dioctahedral Vermiculite, Early Diagenesis, K^+ Fixation, K^+ Selective Sorption, Soil Illitization.

INTRODUCTION

The nature of dioctahedral vermiculite is poorly understood (*e.g.* Douglas, 1989; Moore and Reynolds, 1997). According to the definition given in the report of the Nomenclature Committee of the Association Internationale Pour L'etude Des Argiles (AIPEA) (Guggenheim *et al*., 2006), dioctahedral vermiculite is a dioctahedral 2:1 phyllosilicate with layer charge of between 0.6 and 0.9 per half unit cell and with the interlayers occupied by hydrated cations. This definition is of little use when one plans to analyze natural samples containing dioctahedral vermiculite (*i.e.* soils and freshwater sediments) using XRD. In both soils and freshwater sediments, dioctahedral vermiculite is always associated with other clay minerals, including mixed-layered phases. Determination of the layer charge of the individual phases in such complex mixtures is very difficult if not impossible. Identification of dioctahedral vermiculite in XRD studies is, thus, done using the operational definition of Bailey (1980), Brown and Brindley (1980), Środoń and Gaweł (1988), and Moore and Reynolds (1997) who suggested that vermiculite can be defined as a phase accommodating two planes of water molecules within the interlayer space and giving a 001 peak at ~14 Å when saturated with Mg^{2+} and analyzed in an air-dry state. The peak does not move after solvation with glycerol. In the Na^+-saturated form, dioctahedral vermiculite accommodates one plane of water molecules within the interlayer space and gives a 001 peak at ~12.5 Å when analyzed in an air-dry state. Following solvation with ethylene glycol, the peak moves to ~14 Å, indicating accommodation of one layer of ethylene glycol molecules within the interlayer space.

Dioctahedral vermiculite forms in soils and weathering environments mainly at the expense of dioctahedral mica (muscovite) (Douglas, 1989; Bain *et al*., 1990; Righi *et al*., 1997; Skiba, 2007). The high layer charge in dioctahedral vermiculite is probably inherited from the parent mica and originates mostly from Al-for-Si substitution in the tetrahedral sheet. Depending on the weathering regime, dioctahedral vermiculite may further evolve into dioctahedral smectite-beidellite or hydroxy-interlayered vermiculite (Douglas, 1989; Bain *et al*., 1990; Righi *et al*., 1997; Skiba, 2007). Hydroxy-interlayered vermiculite has an interlayer space which is occupied by an incomplete gibbsite-like octahedral sheet. Dioctahedral vermiculite has been reported in all soil orders, although it has been found more often in soils of cold, temperate, and subtropical climates than in

* E-mail address of corresponding author:
michal.skiba@uj.edu.pl
DOI: 10.1346/CCMN.2013.0610409

soils of other climates (Douglas, 1989). The mineral occurs commonly in soils and fresh sediments (*e.g.* Douglas, 1989; Środoń, 1999, 2003), but has not been reported in sedimentary rocks. Thus, understanding of the evolution of dioctahedral vermiculite during diagenesis is incomplete, although its chloritization involving Mg-hydroxy interlayering and possibly illitization in the marine environment have been suggested (Powers, 1953; Whitehouse and McCarter, 1956; Nelson, 1958, 1962; Malla, 2003).

According to Sawhney (1972), Douglas (1989), and Malla (2003), dioctahedral vermiculite is expected to exhibit strong potential for selective sorption and fixation of cations with low hydration energy, such as K^+, NH_4^+, Cs^+, and Rb^+. Most of the knowledge about the expected properties of dioctahedral vermiculite has been inferred from studies performed on trioctahedral vermiculites. Research by Rich and Black (1964), Page *et al.* (1967), Inoue (1984), and Olk *et al.* (1995) showed that materials containing dioctahedral vermiculite indeed fix K^+. Saturation of dioctahedral vermiculite with K^+ is likely to cause collapse of the interlayers, leading to the formation of a 10 Å illite-like phase. The collapse is expected to be irreversible under the standard ion-exchange procedure described by Jackson (1969).

The aim of the present study was to present evidence for irreversible collapse of dioctahedral vermiculite to a 10 Å illite-like phase after saturation with K^+. The collapse was studied in laboratory experiments simulating conditions found in soils and marine environments. The data presented provide the context for interpreting and discussing the potential evolution of dioctahedral vermiculite in geological environments.

MATERIALS AND EXPERIMENTS

Due to the fact that no dioctahedral vermiculite standard reference material was available, for the purpose of the present study a natural soil sample containing dioctahedral vermiculite was used. Finding an appropriate sample turned out to be quite a difficult task. In most of the studies reporting the occurrence of dioctahedral vermiculite, the XRD data presented were limited to the low-angle region. The behavior of only the strongest (*i.e.* 001) reflection was tested, making the distinction between discrete dioctahedral vermiculite and mixed-layered phases impossible. The potential presence of hydroxyl interlayering (Barnishel and Bertsch, 1989) and intercalation by soil organic matter (Skiba *et. al.*, 2011) made the interpretation of XRD patterns even more ambiguous. Analysis of the available XRD data led to the conclusion that the existence of dioctahedral vermiculite as a discrete mineral has not been proven or well documented.

For the experiments conducted as part of the present study, one Na^+-saturated natural soil clay (*i.e* <2 μm) fraction containing dioctahedral Al-rich vermiculite was selected. The fraction was selected from hundreds of samples analyzed by the author. The sample was taken from the illuvial E (albic) horizon of a podzol found in the Tatra Mountains in southern Poland. The origin of the soil and its properties and mineralogy were described in detail by Skiba (2005, 2007). The sample used (1E) contained a significant amount of dioctahedral illite-vermiculite-smectite (I-V-S) and illite-vermiculite (I-V) mixed-layered minerals, which were rich in vermiculite layers. Beside I-V-S and I-V, the sample also contained kaolinite, illite, and a small amount of quartz. The term illite is used hereafter to describe finely crystalline dioctahedral mica. The clay fraction used was separated from 50 g of the bulk soil material by centrifugation, preceded by removal of organic matter using hydrogen peroxide buffered with Na-acetate buffer, free iron oxide removal according to Mehra and Jackson (1958), and Na^+ saturation. The separated clay fraction was coagulated using NaCl and dialyzed until a conductivity of ~1.2 μS/cm was reached. The suspension obtained was stirred vigorously for 15 min and then split into small

Table 1. Sample symbols, treatments used in the experiments conducted, and potassium and illite-layer concentrations measured in the samples analyzed (%).

Sample	Treatment used	% K	% K_2O	% I, air-dried	% I, EG
(1E)_Na	Na^+ saturation	2.16	2.6	52.38	52.60
(1E)_SW_Na	Artificial sea-water treatment + air-drying + Na^+ saturation	2.94	3.54	68.89	69.95
(1E)_K	K^+ saturation	4.04	4.87	N.A.	N.A.
(1E)_K_Na	K^+ saturation + Na^+ saturation	2.36	2.84	55.45	56.55
(1E)_K_D_Na	K^+ saturation + air-drying + Na^+ saturation	3.09	3.72	72.79	72.66
(1E)_K_T_Na	K^+ saturation + 2 weeks ageing + Na^+ saturation	2.42	2.92	63.07	59.64

% K – potassium concentration measured using flame photometry.
% K_2O – potassium oxide concentration calculated using the measured % K.
% I, air-dried – illite-layer concentration calculated using XRD pattern registered in air-dried conditions.
% I, EG – illite-layer concentration calculated using the XRD pattern registered for samples saturated with ethylene glycol.
N.A. – not analyzed.

https://doi.org/10.1346/CCMN.2013.0610409 Published online by Cambridge University Press

aliquots containing ~300 mg of clay each. The aliquots obtained were treated using different procedures (Table 1).

In order to study the effect of K^+ saturation on the structure of dioctahedral vermiculite (sample (1E)_K_Na), one aliquot of Na^+-saturated sample was saturated with K^+ by repeated washing (four times) using 1 M KCl solution, immediately (*i.e.* without drying) saturated with Na^+, and dialyzed.

In order to study the effect of sample drying on the fixation of K^+ by dioctahedral vermiculite (samples (1E)_K_D_Na), one aliquot of Na^+-saturated sample was saturated with K^+, air dried at room temperature (~20ºC), redispersed, Na^+-saturated, and dialyzed.

The effect of the time of interaction between dioctahedral vermiculite and the K^+-containing solution on interlayer collapse (samples (1E)_K_T_Na) was studied by ageing one aliquot of K^+-saturated sample in a ~50 cm^3 1 M KCl solution for 2 weeks. Following ageing, the sample was Na^+-saturated without drying and then dialyzed.

To simulate the interaction between dioctahedral vermiculite and seawater (samples (1E)_SW_Na) one aliquot of Na^+-saturated sample was dispersed in Instant Ocean® artificial seawater containing ~400 ppm of potassium. The slurry was packed into dialysis tubing and placed in a 5 dm^3 beaker filled with the same artificial seawater. The sample was kept in the system for 4 months. The water in the beaker was changed every few days. The sample in the tubing was shaken from time to time. This procedure allowed the sample to equilibrate with ~250 dm^3 of the artificial seawater. After the treatment, the sample was air dried, redispersed in deionized water, Na^+-saturated, and dialyzed.

The final Na^+ saturation was performed in each case by Na-acetate buffer treatment (1 h at 90ºC) and four washings with 1 M NaCl solution, followed by dialysis. The acetate buffer treatment was used because it appears to be more aggressive than washing with 1 M NaCl and it constitutes a first step in the chemical pre-treatment frequently applied prior to clay fraction separation from natural samples (Jackson, 1969).

ANALYTICAL METHODS

Solid products of the experiments were analyzed using powder XRD. Oriented glass slide mounts with a surface density of ~10 mg/cm^2 clay were prepared from the products by deposition of the clay fractions resuspended in deionized water.

X-ray diffraction analyses were performed using a Philips X'Pert diffractometer (Almelo, The Netherlands) with a vertical goniometer PW3020, equipped with a 1º divergence slit, 0.2 mm receiving slit, incident and diffracted beam Soller slits, 1º anti-scatter slit, and a graphite diffracted-beam monochromator. CuKα radiation was used with an applied voltage of 40 kV and 30 mA current. The mounts were scanned from 2 to 52º2θ at a counting time of 2 s per 0.02º step air-dried in ambient humidity (~20−40 % RH) and after solvation with ethylene glycol.

An attempt was made to evaluate the percentages of the collapsed illite-like interlayers using XRD from oriented mounts based on a whole-pattern multi-specimen modeling technique. The proprietary software, *SYBILLA*, belonging to Chevron, was used for the modeling. *SYBILLA* implements the original algorithms of Drits and Sakharov (1976) in a more user-friendly interface. In the following, I, V, and S denote illite, vermiculite, and smectite layers/interlayers, respectively. A correction for instrumental function was made according to the simplified approach proposed by Reynolds (1986) and Drits (1993) by introducing into the software quantities such as vertical and horizontal beam divergence, goniometer radius, and sample length. The sigma star (σ*) characterizing the distribution of particle orientation was set at 12 for all phases used for the modeling, according to the recommendation of Reynolds (1986). For all layer types, *z* atomic coordinates described by Moore and Reynolds (1997) were used after being modified to fit the layer thickness values used for the modeling. The positions and the amounts of interlayer water and ethylene glycol molecules within smectite and vermiculite interlayers, as proposed by Moore and Reynolds (1997), were used. The K^+ content within illite interlayers was set at 2 atoms per unit cell. The interlayer cation (Ca^{2+}) content for vermiculite and smectite was set at 0.66 and 0.33 atoms per unit cell, respectively. When using *SYBILLA* (version 2.0_Sept 4, 2009), only Ca^{2+} can be introduced as an interlayer cation in expandable phases. Because the modeling was performed for Na^+-saturated samples, a correction designed to account for differences in the scattering factor between Ca^{2+} and Na^+ was made. As the atomic scattering factor is proportional to the number of electrons in the interlayer ion (Reynolds and Reynolds, 1996) and taking into account that Na^+ and Ca^{2+} have 10 and 18 electrons, respectively, the set cation contents (0.66 or 0.33 atoms per unit cell) correspond to approximate values of 0.6 and 0.3 Na^+ atoms per half unit cell. The ordering of the mixed layer modeled was characterized by the Reichweite (R) parameter (Jagodzinski, 1949). R0 denotes randomly interstratified phases, while R1 denotes phases in which the occurrence probability for a given layer type is influenced by the type of the nearest preceding precursor layer. The presence of a superstructure reflection in the XRD data suggested that the R1 phases showed the maximum possible degree of ordering (MPDO). In other words, the successive occurrence of the least abundant layers in R1 phases was prohibited in the stacking. The chemistry and d_{001} spacings used for the modeling were approximated using data from previous studies (Skiba, 2003, 2007) (Table 2). The distribution of coherent scattering

https://doi.org/10.1346/CCMN.2013.0610409 Published online by Cambridge University Press

Table 2. Structural parameters used for modeling of the diferent clay layers.

Layer type	Layer thickness (Å)	Octahedral iron content[a]	Interlayer cation content[d]
Discrete illite	10.02	0.10	1.0
Illite in in I-V-S[c]	9.98	0.10	1.0
Vermiculite (V1w)[b] in V-S[c]	12.38	0.10	0.6
Vermiculite (V1w)[b] in I-V-S[c]	12.50	0.10	0.6
Smectite (S2w)[b]	15.00	0.10	0.3
Vermiculite (V1eg)[b]	13.66	0.08	0.6
Smectite (S2eg)[b]	16.86	0.08	0.3
Kaolinite	7.16	N.A.	N.A.

[a] Number of atoms per half unit cell.
[b] V1w – vermiculite with one layer of water molecules in the interlayer space; V1eg – vermiculite with one layer of ethylene glycol molecules in the interlayer space; S2eg – smectite with two layers of ethylene glycol molecules in the interlayer space.
[c] V-S – vermiculite-smectite mixed-layered minerals; I-V-S – illite-vermiculite-smectite mixed-layer minerals.
[d] Number of monovalent ions per half unit cell.
N.A. – not applicable

domains sizes (CSDSs) was assumed to be lognormal, as described by Drits *et al*. (1997), and was characterized by the mean values (Table 3). The quality of the fit (R_p) was calculated according to the formula given by Howard and Preston (1989):

$$R_p = \frac{\sum_{i=1}^{n} |y_i - y_{ic}|}{\sum_i y_i} \cdot 100 \quad (1)$$

where y_i and y_{ic} are the measured and calculated intensities for the i^{th} point, respectively.

Due to the fact that the automatic genetic algorithm used by *SYBILLA* failed to fit the experimental data, the fitting procedure was performed manually using a trial and error approach. The evaluation was performed for the samples saturated with Na^+ for both air-dried and ethylene glycol-solvated samples independently. Before fitting, the experimental data used were corrected for the presence of quartz by subtraction of the XRD pattern obtained for a quartz standard ground to <2 μm fraction. Although an attempt was made to obtain a satisfactory fit for the whole angular range analyzed, the most attention was paid to obtain a good fit for the most intense reflection around 10–14 Å, as this reflection was found to be the most sensitive to K^+ saturation.

The same material as used in the XRD analysis was used for % K_2O measurements using a Sherwood Model 420 flame photometer (Cambridge, UK). The accuracy of the measurement was verified by K_2O determination in the Plastic Clay NIST standard.

Modeling strategy

The following modeling strategy was established. First the modeling was performed to obtain the best possible fit for the XRD patterns of the Na^+-saturated sample analyzed under air-dry (AD) conditions and after solvation with ethylene glycol (EG). This was done using a mixture of discrete illite and kaolinite with a series of five R0 I-V, one R0 I-V-S, and one R1 I-V. In the AD form under ambient relative humidity conditions (21–40%), the expandable phases studied were dominated by vermiculitic interlayers (*i.e.* interlayers accommodating one layer of water molecules). The influence of dehydrated interlayers potentially existing in the analyzed samples, like that reported for smectites by Ferrage *et al*. (2005, 2007, 2010), appeared to be negligible. This was indicated by the fact that the models obtained for XRD patterns registered for air-dried and EG-saturated samples gave similar results with respect to the vermiculite and smectite percentage. Once comparable results (*i.e.* close quantitative compositions) were obtained for both models, an assumption was made that the models were accurate enough for comparison purposes.

To model the XRD patterns registered for the solid products of the experiments conducted, the models obtained for Na^+-saturated sample were taken as the starting models. In the course of modeling, the structural parameters used (Tables 1 and 2) were kept constant for all the phases except for I-V and I-V-S, for which the starting models were modified by the addition of illite layers in order to obtain the best possible fit with the experimental XRD patterns. The *SYBILLA* software used in this study was unable to keep the percentages of the individual phases fixed. Nevertheless, an attempt was made to obtain a similar concentration for discrete kaolinite, illite, and the individual mixed-layered contributions.

Degree of collapse estimation

The aim of the present study was to evaluate the degree of collapse of interlayer spaces in the starting

https://doi.org/10.1346/CCMN.2013.0610409 Published online by Cambridge University Press

Table 3. Structural parameters used for modeling the XRD patterns of the solid products of the experiments obtained using sample 1E.

Sample	Air-dried RH (%)	R_p (%)	Phases in air[a]	% of each phase	T_{mean}	EG RH (%)	R_p (%)	Phases EG[b]	% of each phase	T_{mean}
(1E)_Na	25	18.76	Kaolinite	11	18	32.30	18.95	Kaolinite	11	18
			I-V R0 (3:97)	9	10			I-V R0 (4:96)	7	10
			I-V R0 (20:80)	6	10			I-V R0 (20:80)	6	10
			I-V-S R0 (3:69:28)	4	10			I-V-S R0 (3:76 :21)	3	10
			I-V R0 (40:60)	12	10			I-V R0 (40:60)	13	10
			I-V R0 (61:39)	8	10			I-V R0 (61:39)	7	10
			I-V R0 (83:17)	35	10			I-V R0 (80:20)	38	10
			Illite	9	14			Illite	9	14
			I-V R1 (60:40)	6	10			I-V R1 (60:40)	6	10
(1E)_K_Na	28.80	18.68	Kaolinite	11	18	25.70	21.48	Kaolinite	11	18
			I-V R0 (8:91)	9	10			I-V R0 (4:96)	7	10
			I-V R0 (33:67)	5	10			I-V R0 (33:67)	6	10
			I-V-S R0 (15:66:19)	6	10			I-V-S R0 (15:66:19)	3	10
			I-V R0 (53:47)	11	10			I-V R0 (53:47)	12	10
			I-V R0 (67:33)	5	10			I-V R0 (67:33)	8	10
			I-V R0 (80:20)	37	10			I-V R0 (80:20)	37	10
			Illite	11	14			Illite	11	14
			I-V R1 (60:40)	5	10			I-V R1 (60:40)	5	10
(1E)_K_T_Na	29	18.39	Kaolinite	8	18	24.80	19.55	Kaolinite	10	18
			I-V R0 (8:92)	4	10			I-V R0 (8:92)	5	10
			I-V R0 (29:71)	10	10			I-V R0 (29:71)	12	10
			I-V-S R0 (2:77:21)	3	10			I-V-S R0 (2:77:21)	3	10
			I-V R0 (59:41)	16	10			I-V R0 (59:41)	10	10
			I-V R0 (67:33)	3	10			I-V R0 (67:33)	4	10
			I-V R0 (87:13)	39	10			I-V R0 (87:13)	40	10
			Illite	11	14			Illite	9	14
			I-V R1 (66:34)	6	10			I-V R1 (66:34)	7	10
(1E)_K_D_Na	23.40	21.63	Kaolinite	10	18	28	22.95	Kaolinite	10	18
			I-V R0 (40:60)	5	10			I-V R0 (40:60)	5	10
			I-V R0 (60:40)	6	10			I-V R0 (60:40)	6	10
			I-V R0 (80:20)	52	10			I-V R0 (80:20)	54	10
			Illite	17	10			Illite	16	10
			Illite	9	14			Illite	9	14
1ESW	42	19.45	Kaolinite	10	18	24.40	19.45	Kaolinite	9	18
			I-V R0 (20:80)	3	10			I-V R0 (20:80)	3	10
			I-V R0 (59:41)	23	10			I-V R0 (59:41)	20	10
			I-V R0 (80:20)	31	10			I-V R0 (80:20)	32	10
			I-V R0 (90:10)	16	10			I-V R0 (90:10)	18	10
			Illite	9	14			Illite	10	14
			Illite	7	10			Illite	7	10

RH – relative humidity measured during XRD analysis
R_p – parameter describing the goodness of fit
[a] I – illite, V – vermiculite (accomodating one layer of water molecules within the interlayer space), S – smectite (accommodating two layers of water molecules within the interlayer space; R0 and R1 denote random and ordered (exhibiting MPDO) mixed-layer phases, respectively; numbers in parentheses denote relative proportions of illite *vs.* vermiculite *vs.* smectite within individual mixed-layer minerals.
EG – ethylene glycol-solvated samples
[b] I – illite, V – vermiculite (accommodating one layer of ethylene glycol molecules within the interlayer space), S – smectite (accommodating two layers of ethylene glycol molecules within the interlayer space; R0 and R1 denote random and ordered (exhibiting MPDO) mixed-layer phases, respectively; numbers in parentheses denote relative proportions of illite *vs.* vermiculite *vs.* smectite within individual mixed-layer minerals.
T_{mean} – the mean cystallite thickness in a given number of layers.

materials produced by different treatments used in the experiments conducted. The evaluation was performed by the comparison of the concentration of illite-like phases calculated for samples using models obtained for fitted XRD patterns *via* the following formula:

$$\%\mathrm{I} = C_\mathrm{I} + \sum_{i=1}^{n} C_\mathrm{I}^{\mathrm{IV}i} \quad (2)$$

where C_I is the weight concentration of illite in the given sample. $C_\mathrm{I}^{\mathrm{IV}i}$ is the weight concentration of illite contained in a given (i^{th}) I-V or I-V-S in the given sample. $C_\mathrm{I}^{\mathrm{IV}i}$ was calculated according to the following formula:

$$C_\mathrm{I}^{\mathrm{IV}i} = \frac{C_{\mathrm{IV}i} M_\mathrm{I} W_\mathrm{I}^{\mathrm{IV}i}}{(M_\mathrm{I} W_\mathrm{I}^{\mathrm{IV}i} + M_\mathrm{V} W_\mathrm{V}^{\mathrm{IV}i})} \quad (3)$$

where $C_{\mathrm{IV}i}$ is the weight concentration of a given (i^{th}) I-V or I-V-S in the sample and M_I and M_V are the molecular weights of illite and expandable layers, respectively. $W_\mathrm{I}^{\mathrm{IV}i}$ is the percentage of illite, while $W_\mathrm{V}^{\mathrm{IV}i}$ is the percentage of expandable layers in a given (i^{th}) I-V or I-V-S. Molecular weights of components were approximated assuming the following simplified formulae: $KAl_2^{VI}Al^{IV}Si_3O_{10}(OH)_2$ for illite, $Na_{0.6}Al_2^{VI}Al_{0.6}^{IV}Si_{3.4}O_{10}(OH)_2{\cdot}2H_2O$ for vermiculite with one H_2O plane, $Na_{0.3}Al_2^{VI}Al_{0.3}^{IV}Si_{3.7}O_{10}(OH)_2{\cdot}4H_2O$ for smectite with two H_2O planes, $Na_{0.6}Al_2^{VI}Al_{0.6}^{V}Si_{3.4}O_{10}(OH)_2{\cdot}C_2H_4(OH)_2$ for vermiculite with one EG plane, and $Na_{0.3}Al_2Al_{0.3}Si_{3.7}O_{10}(OH)_2{\cdot}2C_2H_4(OH)_2$ for smectite with two EG planes. The formulae were simplified because no information was available on the layer charge of the components. The number of water and glycol molecules was assumed according to Bradley and Weiss (1961).

RESULTS AND INTERPRETATION

Qualitative description of experimental XRD patterns and the results of chemical analysis.

The XRD patterns of the sample saturated with Na^+ ((1E)_Na) obtained under air-dry conditions showed the presence of peaks belonging to different I-V and I-V-S at ~22.5 Å, ~12.5 Å, ~6 Å, 3.34–3 Å, and ~2 Å (Figure 1a). Following the solvation of the sample with ethylene glycol, I-V and I-V-S gave peaks at ~24 Å, ~14 Å, 5–4.5 Å, ~3.3 Å, and ~2 Å (Figure 1b). Peaks at ~7 Å and 3.58 Å belonged to kaolinite, while sharp reflections at 3.34 Å and 4.26 Å belonged to quartz. Reflections at 10 Å together with higher-order peaks at, 5 Å, 2.5 Å, and ~3.33 Å indicated the presence of illite. The peak at 4.47 Å is the 02l band from dioctahedral phyllosilicates, resulting from imperfect orientation in the 'oriented' clay film.

The XRD pattern of the K^+-saturated sample showed the presence of a series of reflections from the 10 Å

https://doi.org/10.1346/CCMN.2013.0610409 Published online by Cambridge University Press

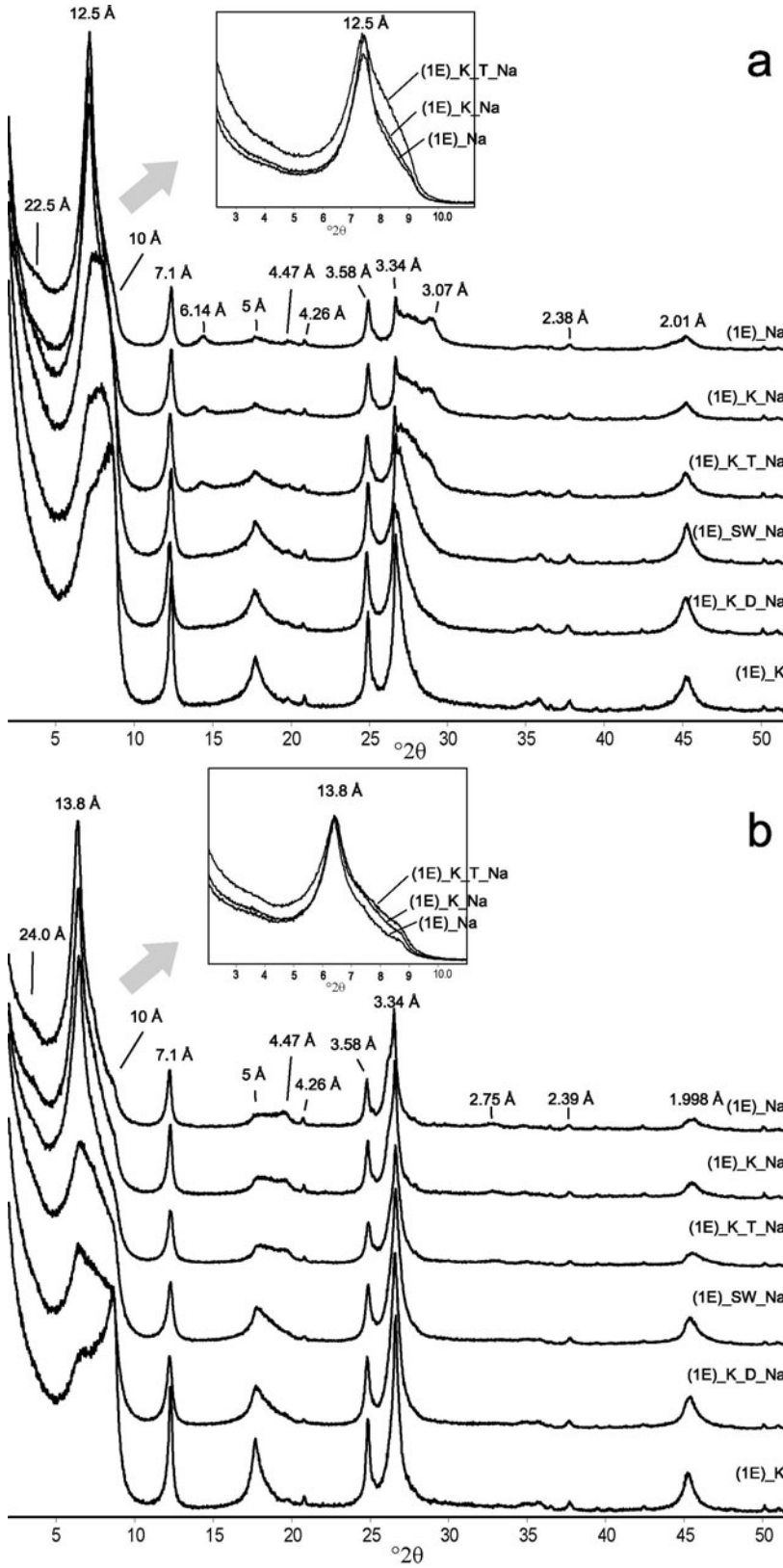

Figure 1. Comparison between XRD patterns registered for the 1E sample treated using different procedures (Table 1): (a) air dried; and (b) ethylene glycol solvated.

https://doi.org/10.1346/CCMN.2013.0610409 Published online by Cambridge University Press

phase (Figure 1) indicating the collapse to 10 Å of the vermiculite interlayers present in the sample (*e.g.* Sawhney, 1972; Douglas, 1989; Moore and Reynolds, 1997; Malla, 2003). The low-angle tail observed for the 10 Å reflection indicated the presence of some hydrated interlayers.

The XRD patterns of the sample that was K^+-saturated and immediately (*i.e.* without drying) Na^+-saturated showed little change relative to the XRD pattern of the starting materials: a decrease in the intensity of low-angle reflections relative to higher-angle reflections was noted (Figure 1). This behavior indicated that K^+ saturation itself (*i.e.* without drying) caused collapse to 10 Å of at least a small portion of initially hydrated interlayers present in the sample. This interpretation was supported by the results of chemical analysis, as the potassium concentration in sample (1E)_K_Na was greater than the potassium concentration in sample (1E)_Na (Table 1). In other words, K^+ saturation without drying of the sample resulted in the fixation of a limited amount of K^+, leading to the collapse of a small proportion of the interlayers. The collapse was irreversible under the standard ion-exchange procedure used here.

In the XRD pattern of sample (1E)_K_T_Na, a further decrease (relative to sample (1E)_K_Na) in the intensity of the low-angle reflections relative to the higher-angle reflections was observed (Figure 1). This observation was consistent with the results of chemical analysis (Table 1), showing that sample (1E)_K_T_Na contained more K^+ than sample (1E)_K_Na. This behavior indicated that in the case of sample (1E)_K_T_Na, the longer time of reaction with the K^+-bearing solution produced more collapsed interlayers (Figure 1, Table 1) than the shorter time of reaction.

The XRD patterns registered under air-dry conditions for a sample that was K^+-saturated, air dried, and saturated with Na^+ ((1E)_K_D_Na) showed intense reflections at 10 Å, 5 Å, 3.33 Å, and 2 Å (Figure 1a). The reflections did not change position following EG solvation (Figure 1b), indicating the presence of a 10 Å illite-like phase. The sample contained some swelling phases, as indicated by the presence of a broad reflection at ~14 Å in the XRD pattern of the EG-solvated sample. The XRD patterns of the sample treated with artificial seawater (1E)_SW_Na was very similar to the pattern of the (1E)_K_D_Na sample. The ratio between the intensities of reflections belonging to 10 Å phases and reflections belonging to swelling phases indicated that sample (1E)_SW_Na contained less of the illite-like phase than sample (1E)_K_D_Na. The results of chemical analysis supported this interpretation (Table 1), as the K^+ concentration in sample (1E)_K_D_Na was greater than the K^+ concentration in sample (1E)_SW_Na. The introduction of an air drying step between K^+ saturation and ion exchange caused the fixation of a significant portion of K^+, leading to the collapse of the vermiculite interlayers (Figure 1, Table 1). The treatment involving reaction with artificial seawater also caused a collapse of a significant number of vermiculite interlayers (Figure 1, Table 1).

Quantitative description of the experimental XRD patterns

The XRD patterns of the starting sample were modeled using a complex mixture of discrete kaolinite, illite with several I-V, and I-V-S with R_p values ranging from 18.4 to 23% (Table 3, Figure 2). As shown in a previous study (Skiba, 2007), the sample can be described with a minimum of four swelling contributions. The detailed modeling performed as part of the present study showed that four mixed-layered contributions were insufficient to fit the XRD patterns. To obtain a satisfactory fit of the low-angle regions, seven mixed-layered structures were necessary (Figure 3). The R0 I-V-S structure was added to fit the low-angle tails of the main peaks at ~12.5 Å and 14 Å in an air-dry and ethylene glycol-solvated state, respectively. The R1 I-V structure was taken into account during the fitting because of the presence of super-structure reflections at ~22.5 Å and ~24 Å in the patterns registered for the air-dry and ethylene glycol-solvated samples, respectively. The need for the use of a complex set of mixed-layered structures was also indicated by the presence in the XRD pattern of the air-dried sample of a broad asymmetric reflection between the 003 illite peak at 3.33 Å and the 004 vermiculite peak at ~3 Å (Figure 3). This reflection is probably the sum of a set of narrower reflections. By applying the Méring Principle (Méring, 1949) one may conclude that the reflections belong to the I-V, with the composition between discrete illite and almost discrete vermiculite. The broad reflection was, at least to some extent, approximated using the set of seven mixed-layered structures (Figure 3).

The XRD patterns of samples (1E)_K_Na and (1E)_K_T_Na were fitted using the same complex models (*i.e.* I + K + 7 mixed-layered structures) as the patterns used for the fitting of the starting (1E)_Na sample. The models obtained for samples (1E)_K_Na and (1E)_K_T_Na showed the same concentration of individual phases as the (1E)_Na sample. The fit was obtained (as expected) by increasing the concentration of illite layers within individual mixed-layered structures (Table 3).

Three mixed-layered structures, kaolinite, and two populations of illite were needed to fit the XRD patterns of sample (1E)_K_D_Na. The XRD patterns of sample (1E)_SW_Na were fitted using a mixture of kaolinite, four mixed-layered structures, and two populations of illite. This was because most of the mixed-layered minerals initially present in the sample were transformed into an 'illite like' phase (*i.e.* I or R0 >0.8 I-V) due to K^+ fixation.

The quality of the fit obtained for all the XRD patterns presented in this study is generally low

https://doi.org/10.1346/CCMN.2013.0610409 Published online by Cambridge University Press

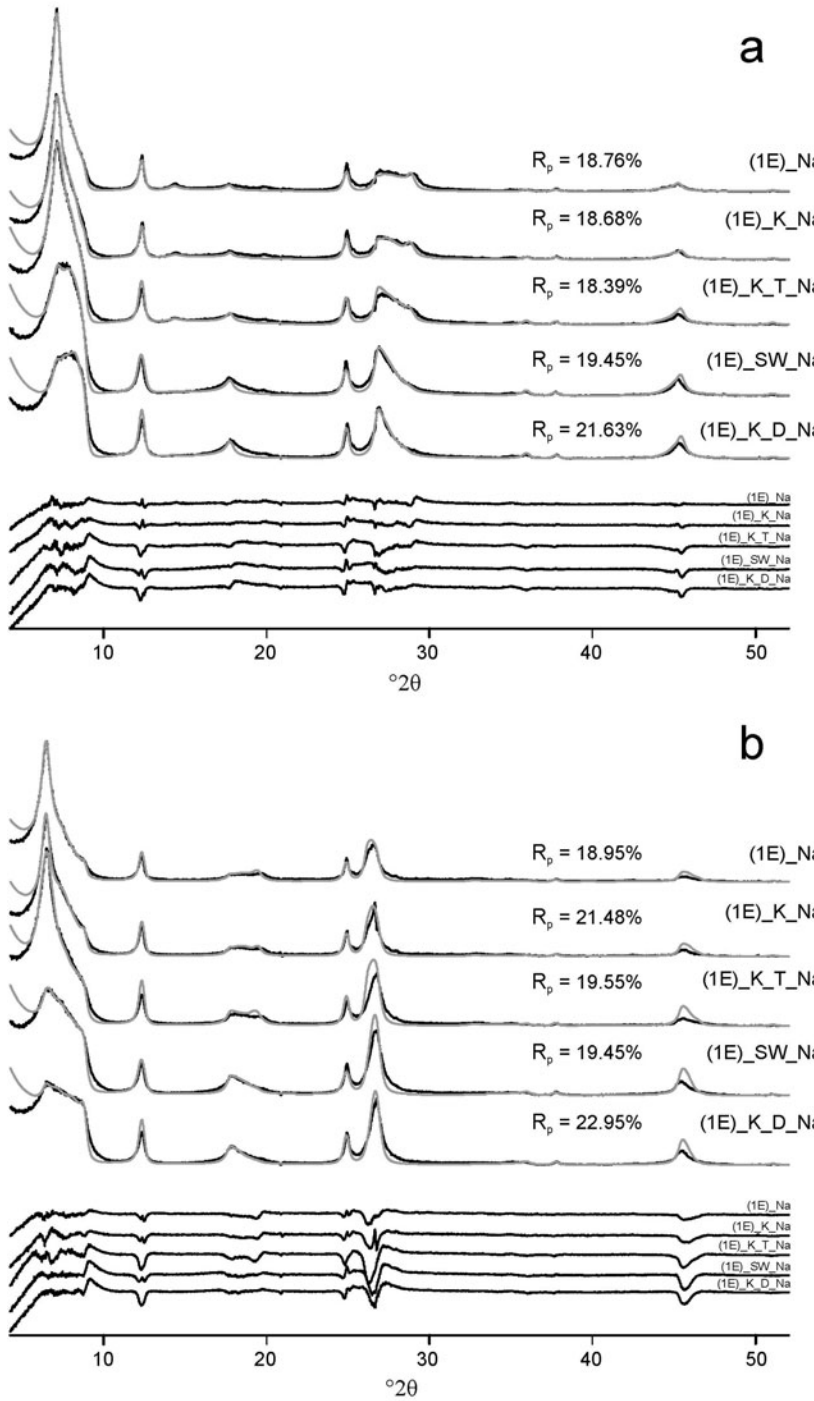

Figure 2. Experimental (black) and calculated (gray) XRD patterns of the solid products of the experiments conducted (Table 1) using sample 1E: (a) air dried; and (b) ethylene glycol solvated. Difference plots are shown at the bottom of each figure.

(Table 3) when compared with the results of other researchers (*e.g.* Claret *et al.*, 2004; Hubert *et al.*, 2009; Lanson *et al.*, 2009) This is probably due to a weak orientation of the samples in the mounts, as indicated by the presence of *hk* bands within XRD patterns (Figures 1 and 2). The poor fit also indicates the weakness of the models used for the modeling of such complex mixtures. The results of the modeling can only be treated as a rough approximation of the actual phase composition of the samples analyzed.

The percentages of illite (%I) obtained using XRD correlate linearly with the K_2O concentrations measured

https://doi.org/10.1346/CCMN.2013.0610409 Published online by Cambridge University Press

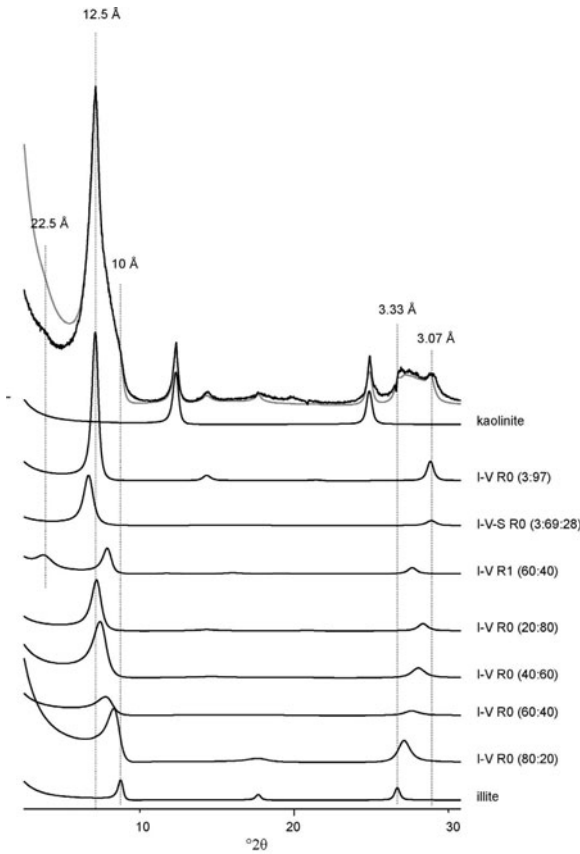

Figure 3. Elementary contributions to the model obtained for the XRD pattern registered for the air-dried (1E)_Na sample.

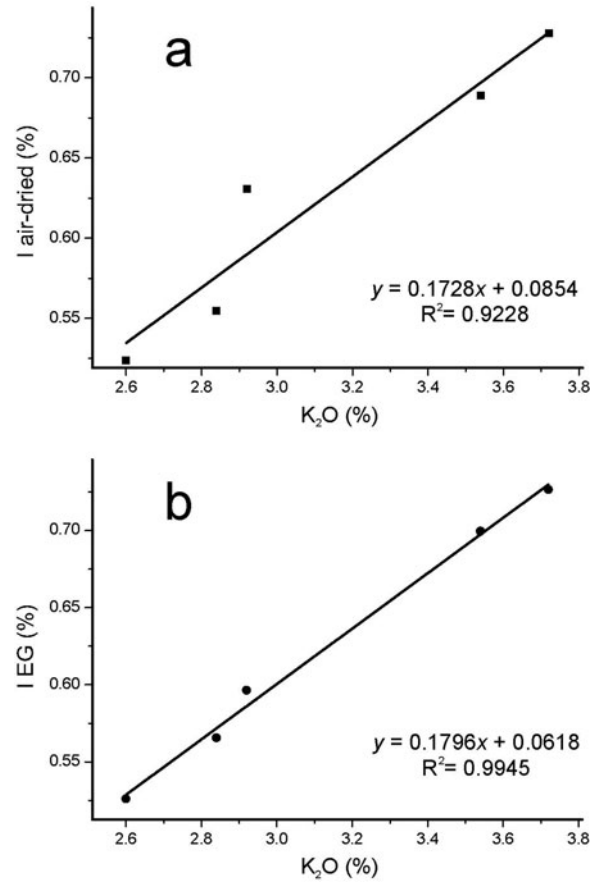

Figure 4. Correlation between the K_2O concentration and the percentage of illite (% I) calculated for the products of the experiments conducted using sample 1E: (a) % I calculated using the models obtained for the air-dried samples; and (b) % I calculated using the models obtained for the ethylene glycol-solvated samples.

by flame photometry (Figure 4). The coefficients of determination (R^2) for the correlations of K_2O *vs.* % I calculated from both air-dried and ethylene glycol-solvated models exceed 0.9 (Figure 4), indicating that the models obtained illustrate the observed tendencies well.

DISCUSSION

Collapse of interlayers following K^+ saturation.

The results obtained indicate that K^+ saturation causes the collapse of dioctahedral vermiculite to the 10 Å phase. Without drying the K^+-saturated dioctahedral vermiculite, most of the interlayers can be exchanged with Na^+ (*i.e.* re−opened) using the standard ion-exchange procedure (Jackson ,1969). When drying is applied to K^+-saturated dioctahedral vermiculite, most of the K^+ present in the interlayer spaces becomes fixed (*i.e.* cannot be exchanged with other cations using the standard procedure). The fixation results in the collapse of dioctahedral vermiculite to a 10 Å illite-like phase. Because the collapse is irreversible under the standard ion-exchange procedure, the 10 Å phase formed is practically indistinguishable from illite. Assuming that the accepted definition of dioctahedral vermiculite (Guggenheim *et. al.*, 2006) is correct, the material is expected to have the same layer charge and composition as aluminous illite. This is consistent with the results of Scott and Reed (1964) obtained for muscovite exchanged with Na^+ without modification of the layer charge. The exchanged muscovite exhibited the XRD pattern characteristic of dioctahedral vermiculite. Barshad (1950) also reported that very finely ground sodium mica paragonite with a negative layer charge ~1 eq per half unit cell gave a 001 reflection at ~12.9. Å, which is indicative of Na^+-saturated vermiculte according to Brown and Brindley (1980).

From the results obtained for the sample that was aged in K^+-bearing solution for 2 weeks before being Na^+-saturated, whether or not time had had a significant effect on the degree of irreversible collapse is unclear. An increase in the concentration of fixed K^+ and illite layers in sample (1E)_K_T_Na relative to sample (1E)_K_Na was observed. This suggests that the time of reaction with K^+-bearing solutions is a possible factor affecting the degree of dioctahedral vermiculite collapse.

https://doi.org/10.1346/CCMN.2013.0610409 Published online by Cambridge University Press

Despite the fact that in the present study the collapse of dioctahedral vermiculite was achieved in simplified systems, the results obtained can, at least to some extent, be used in the discussion of possible processes of dioctahedral vermiculite transformation in soils. Dioctahedral vermiculite formed in different soil orders at the expense of dioctahedral mica (by mica opening) is likely to be reclosed when the K^+ concentration increases (*e.g.* due to the weathering of K^+-bearing mineral grains). This conclusion is supported by the results of previous field and greenhouse studies showing extensive K^+ fixation in vermiculitic soils treated with potassium fertilizers (Page *et al.*, 1963, 1967; Olk *et al.*, 1995; Simonsson *et al.*, 2009). Additionally, Simonsson *et al.* (2009) showed that fixation is accompanied by the formation of a 10 Å illite-like phase. Fixation of K^+ by weathered muscovite in soils of Pennsylvania was also indicated by Price *et al.* (2008). Soils are extremely heterogeneous systems containing different chemical microenvironments, in which the potential for dioctahedral mica opening (vermiculitization) and dioctahedral vermiculite reclosing ('illitization') may exist next to each other. Dioctahedral vermiculite formed at one site within a soil profile may (*e.g.* due to biogenic activity) become translocated into a microenvironment with the potential for dioctahedral vermiculite reclosing. In most soils, however, the process of dioctahedral mica vermiculitization probably prevails over potential dioctahedral vermiculite reclosing. This is indicated by the fact that soils contain dioctahedral vermiculite. Vermiculitization is probably due to K^+ uptake by plants and other living organisms in the soil.

The collapse of dioctahedral vermiculite caused by K^+ saturation and dehydration of the interlayer space is a likely mechanism for so-called 'soil illitization' reported by Berkgaut *et al.* (1994) and Righi *et al.* (1995). The previously proposed mechanism involving cyclic wetting and drying of K^+-saturated smectite appears to be well documented (Eberl *et al.*, 1986). Both dioctahedral vermiculite reclosing and smectite contraction can probably contribute to soil illite formation. In soils of climates other than arid and semi-arid, dioctahedral vermiculite reclosing appears to be more likely to occur than wetting- and drying-driven 'illitization' of smectite due to the fact that the soils are relatively rich in dioctahedral vermiculite (Douglas, 1989) and drying is not very frequent in such climates.

Reaction with artificial seawater

The proposed mechanism involving dioctahedral vermiculite reclosing due to a local increase in K^+ is likely to be responsible for the formation of young illite in soils reported by Berkgaut *et al.* (1994) and Righi *et al.* (1995), but does not explain the almost complete lack of dioctahedral vermiculite in sea sediments and sedimentary rocks. The increase in the number of irreversibly collapsed (*i.e.* to 10 Å) interlayers and in the amount of fixed K^+ in the samples treated for 4 months with artificial seawater indicates that K^+ is adsorbed selectively by dioctahedral vermiculite from seawater.

A significant number of collapsed interlayers was likely to be 'artificially' produced by sample drying. However, at least a small portion of the K^+ adsorbed was likely to be fixed before drying as indicated above. Sample dehydration (air drying, oven drying, or freeze drying) is a first step in the standard procedure commonly applied to marine sediment samples. Observed selective K^+ sorption, together with the drying of collected samples, is probably responsible for the fact that dioctahedral vermiculite has not been reported in marine sediments and sedimentary rocks. Natural dehydration of sediments also takes place in diagenesis.

The results obtained for the samples treated with artificial seawater reported here differ significantly from the results obtained by Whitehouse and McCarter (1956) who reported the chloritization of smectite treated for 6–60 months with artificial seawater. The chloritization occurred due to the selective uptake of Mg^{2+} and the formation of Mg-hydroxy interlayering. The difference is probably because Whitehouse and McCarter (1956) conducted their experiment in a closed system (*i.e.* they used 1 dm^3 of artificial seawater/2 g of the sample) with limited K^+ availability, while the experiment described in the present study was a semi-open system experiment (*i.e.* 250 dm^3 of artificial seawater/1 g of the sample was used). This suggestion is supported by the fact that chloritization of soil-derived dioctahedral vermiculite was reported as being the main early diagenetic process in estuary sediments of the Rappahanock River by Nelson (1958, 1962) and the Chesapeake Bay area by Powers (1953). In both cases, the sedimentation regime (*i.e.* coagulation and fast deposition of river loads) limited the contact of the deposited clays with open sea waters. Nelson (1958) noted that in estuary sediments deposited in more saline (~20‰ TDS) waters, the chlorite and illite content increased while the content of dioctahedral vermiculite decreased, which may suggest the presence of both chloritization and illitization of dioctahedral vermiculite. The selective sorption of K^+ from seawater by dioctahedral vermiculite documented in the present study is consistent with a suggestion made by Malla (2003) who stated that dioctahedral vermiculite transforms into dioctahedral mica in marine environments.

Reasons for the lack of dioctahedral vermiculite in sediments and sedimentary rocks

Early diagenetic illitization and chloritization of dioctahedral vermiculite are likely reasons for dioctahedral vermiculite not being found in sediments and sedimentary rocks. According to available data on dioctahedral mica weathering (*e.g.* Righi *et al.*, 1997; Skiba, 2007), dioctahedral vermiculite appears to be a

https://doi.org/10.1346/CCMN.2013.0610409 Published online by Cambridge University Press

kind of transient alteration phase of dioctahedral mica toward smectite. In addition, the fact that the XRD patterns of the (1E)_Na sample were fitted using a complex mixture of mixed-layered structures containing I, V, and S supports this suggestion. The reason for the occurrence of dioctahedral vermiculite being confined to soils could very well be because soils are relatively young environments where a transient phase can be observed. This argument, however, would not explain the lack of the material in a state of transition and containing dioctahedral vermiculite in sediments and sedimentary rocks. Water erosion washing out soil material containing dioctahedral vermiculite is expected to be a common phenomenon in areas where dioctahedral vermiculite is formed. If the transformation of dioctahedral vermiculite did not occur somewhere between the erosion stage and the diagenesis stage, then the presence of the mineral in sediments and sedimentary rocks would be expected.

CONCLUSIONS

Dioctahedral vermiculite collapses irreversibly at room temperature to a 10 Å illite-like phase when saturated with K^+. The observed collapse indicates that the process of K^+ fixation leading to dioctahedral vermiculite contraction ('illitization') is very likely to occur in soils and weathering environments (*e.g.* due to local fluctuation in K^+ concentration). Both the collapse of dioctahedral vermiculite and the contraction of smectite due to wetting and drying are likely to contribute to soil-illite formation. Dioctahedral vermiculite adsorbs K^+ from seawater selectively. 'Illitization' of dioctahedral vermiculite is very likely to occur in the early diagenesis of open systems in marine environments where sediments have unlimited contact with seawater. The potentially existing processes in nature (*i.e.* soil and early diagenetic 'illitization') together with early diagenetic chloritization are probably responsible for the lack of dioctahedral vermiculite in marine sediments and sedimentary rocks. These processes need to be taken into consideration in sedimentary-basin studies when evaluating detrital input into the basins.

ACKNOWLEDGMENTS

The present research was supported by the Polish Ministry of Science and Higher Education Grant No. NN 305 379238. Chevron ETC and Douglas McCarty are acknowledged for their permission to use their proprietary *SYBILLA* software. The authors thank Joseph W. Stucki, Motoharu Kawano, Javier Cuadros, and the four anonymous reviewers for critical reading of the manuscript and for the constructive suggestions and comments. Grzegorz Zebik improved the English.

REFERENCES

Bailey, S.W. (1980) Structures of Layer Silicates. Pp. 2–124 in: *Crystal Structures of Clay Minerals and their X-ray Identification* (G.W. Brindley and G. Brown, editors). Monograph 5, Mineralogical Society, London.

Bain, D.C., Mellor, A., and Wilson, M.J. (1990) Nature and origin of an aluminous vermiculitic weathering product in acid soils from upland catchments in Scotland. *Clay Minerals*, **25**, 467–475.

Barnishel, R.I. and Bertsch, P.M. (1989) Chlorites and hydroxy-interlayered vermiculite and smectite. Pp. 729–788 in: *Minerals in Soil Environments*, *2nd edition* (J.B. Dixon and S.B. Weed, editors). Soil Science Society of America, Madison, Wisconsin, USA.

Barshad, I. (1950) The effect of the interlayer cations on the expansion of the mica type of crystal lattice. *American Mineralogist*, **35**, 225–238.

Berkgaut, V., Singer, A., and Stahr, K. (1994) Palagonite reconsidered: Paracrystalline illite-smectites from regoliths on basic pyroclastics. *Clays and Clay Minerals*, **42**, 582–592.

Bradley, W.F. and Weiss, E.J. (1961) A glycol-sodium vermiculite complex. *Clays and Clay Minerals*, **10**, 117–122.

Brown, G. and Brindley, G.W. (1980) X-ray diffraction procedures for clay mineral identification. Pp. 305–360 in: *Crystal Structures of Clay Minerals and their X-ray Identification* (G.W. Brindley and G. Brown, editors). Monograph **5**, Mineralogical Society, London.

Claret, F., Sakharov, B.A., Drits, V.A., Velde, B., Meunier, A., Griffault, L., and Lanson, B. (2004) Clay minerals in the Meuse-Haute Marne underground laboratory (France): possible influence of organic matter on clay mineral evolution. *Clays and Clay Minerals*, **52**, 515–532.

Douglas, L.A. (1989) Vermiculites. Pp. 635–668 in: *Minerals in Soil Environments* (J.B. Dixon and S.B. Weed, editors). Soil Science Society of America, Madison, Wisconsin, USA.

Drits, V.A. and Sakharov, B.A. (1976) *X-ray Analysis of Mixed-layered Clay Minerals*. Nauka, Moscow (in Russian).

Drits, V.A., Weber, F., Salyn, A.L., and Tsipursky, S.L. (1993) X-ray identification of one-layer illite varieties: Application to the study of illites around uranium deposits of Canada. *Clays and Clay Minerals*, **41**, 389–398.

Drits, V.A., Środoń, J., and Eberl, D.D. (1997) XRD measurements of mean crystallite thickness of illite and illite/smectite: reappraisal of the Kübler index and the Scherrer equation. *Clays and Clay Minerals*, **45**, 461-475.

Eberl, D.D., Środoń, J., and Northrop, H.R. (1986) Potassium fixation in smectite by wetting and drying. Pp. 296–326 in: *Geochemical Processes at Mineral Surfaces* (J.A. Davis and K.F. Hayes, editors). American Chemical Society Symposium Series, v. **323**.

Ferrage, E., Lanson, B., Sakharov, B.A., and Drits, V.A. (2005) Investigation of smectite hydration properties by modeling experimental X-ray diffraction patterns: Part I. Montmorillonite hydration properties. *American Mineralogist*, **90**, 1358–1374.

Ferrage, E., Lanson, B., Sakharov, B.A., Geoffroy, N., Jacquot, E., and Drits, V.A. (2007) Investigation of dioctahedral smectite hydration properties by modeling of X-ray diffraction profiles: Influence of layer charge and charge location. *American Mineralogist*, **92**, 1731–1743.

Ferrage, E., Lanson, B., Michot, L.J., and Robert, J.L. (2010) Hydration properties and interlayer organization of water and ions in synthetic Na-smectite with tetrahedral layer charge. Part 1. Results from X-ray diffraction profile modeling. *Journal of Physical Chemistry C*, **114**, 4515–4526.

Guggenheim, S., Adams, J.M., Bain, D.C., Bergaya, F., Brigatti, M.F., Drits, V.A., Formoso, M.L.L., Galán, E., Kogure, T., and Stanjek, H. (2006) Summary of recommen-

dations of nomenclature committees relevant to clay mineralogy: report of the Association Internationale pour L'Etude des Argiles (AIPEA) Nomenclature committee for 2006. *Clays and Clay Minerals*, **54**, 761–772.

Howard, S.A. and Preston, K.D. (1989) Profile fitting of powder diffraction patterns. Pp. 217–275 in: *Modern Powder Diffraction* (D.L. Bish and J.E. Post, editors). Mineralogical Society of America, Chantilly, Virginia, USA.

Hubert, F., Caner, L., Meunier, A., and Lanson, B. (2009) Advances in the characterization of soil clay mineralogy using X-ray diffraction: from decomposition to profile fitting. *European Journal of Soil Science*, **60**, 1093–1105.

Inoue, A. (1984) Thermodynamic study of Na-K-Ca exchange reactions in vermiculite. *Clays and Clay Minerals*, **32**, 311–319.

Jackson, M.L. (1969) *Soil Chemical Analysis. Advanced Course*, 2nd edition. Published by the author, Madison, Wisconsin.

Jagodzinski, H. (1949) Eindimensionale fehlordnung in kristallen und ihr einfluss auf die Röntgeninterferenzen: I Berechnung des fehlordnungsgrades aus der Röntgenintensitaten. *Acta Crystallographica*, **2**, 201–207.

Lanson, B., Sakharov, B.A., Claret, F., and Drits, V.A. (2009) Diagenetic smectite-to-illite transition in clay-rich sediments: a reappraisal of X-ray diffraction results using the multi-specimen method. *American Journal of Science*, **309**, 476–516.

Malla, P.B. (2003) Vermiculite. Pp. 766–769 in: *Encyclopedia of Sediments and Sedimentary Rocks* (G. Middleton, editor). Springer, Dordrecht, Germany.

Mehra, O.P. and Jackson, M.L. (1958) Iron oxide removal from soils and clays by dithionite-citrate system buffered with sodium bicarbonate. *Clays and Clay Minerals*, **7**, 317–327.

Méring, J. (1949) L'Inté reference des rayons X dans les systems à stratification dé sordonnée. *Acta Crystallographica*, **2**, 371–377.

Moore, D.M. and Reynolds, R.C. (1997) *X-ray Diffraction and the Identification and Analysis of Clay Minerals*. Oxford University Press, Oxford, New York.

Nelson, B.W. (1958) Clay Mineralogy of the bottom sediments Rappahannock River, Virginia. *Clays and Clay Minerals*, **7**, 135–147.

Nelson, B.W. (1962) Clay mineral diageneis in the Rappahannock Estuary: an explanation. *Clays and Clay Minerals*, **11**, 210.

Olk, D.C., Cassman, K.G., and Carlson, R.M. (1995) Kinetics of potassium fixation in vermiculitic soils under different moisture regimes. *Soil Science Society of America Journal*, **59**, 423–429.

Page, A.L., Bingham, F.T., Ganje, T.J., and Garber, M.J. (1963) *Soil Science Society of America Proceedings*, **27**, 323–326.

Page, A.L., Burge, W.D., Ganje, T.J., and Garber, M.J. (1967) Potassium and ammonium fixation by vermiculitic soils. *Soil Science Society of America Proceedings*, **31**, 337–341.

Powers, M.C. (1953) Clay diagenesis in the Chesapeake Bay area. *Clays and Clay Minerals*, **2**, 68–80.

Price, J.R., Heitmann, N., Hull, J., and Szymański, D. (2008) Long-term average mineral weathering rates from watershed geochemical mass balance methods: Using mineral modal abundances to solve more equations in more unknowns. *Chemical Geology*, **254**, 36–51.

Reynolds, R.C (1986) The Lorentz-polarization factor and preferred orientation in oriented clay aggregates. *Clays and Clay Minerals*, **34**, 359–367.

Reynolds, R.C. and Reynolds, R.C. III (1996) *Newmod for Windows*. The calculation of one-dimensional X-ray diffraction patterns of mixed-layered clay minerals. Hanover, New Hampshire, USA, 25 pp.

Rich, C.I. and Black, W.R. (1964) Potassium exchange as affected by cation size, pH, and mineral structure. *Soil Science*, **97**, 384–390.

Righi, D., Velde, B., and Meunier, A. (1995) Clay stability in clay-dominated soil systems. *Clay Minerals*, **30**, 45–54.

Righi, D., Räisänen, M.L., and Gillot, F. (1997) Clay mineral transformations in podzolized tills in central Finland. *Clay Minerals*, **32**, 531–544.

Sawhney, B.L. (1972) Selective sorption and fixation of cations by clay minerals: a review. *Clays and Clay Minerals*, **20**, 93–100.

Scott, A.D. and Reed, M.G. (1964) Expansion of potassium-depleted muscovite. *Clays and Clay Minerals*, **13**, 247–261.

Simonsson, M., Hillier, S., and Öborn, I. (2009) Changes in clay minerals and potassium fixation capacity as a result of release and fixation of potassium in long-term field experiments. *Geoderma*, **151**, 109–120.

Skiba, M. (2003) Mineralogiczno-geochemiczne aspekty procesu bielicowania w glebach rozwiniętych na skalach krystalicznych w Tatrach. PhD thesis, Jagiellonian University, Kraków, Poland, 110 pp.

Skiba, M. (2007) Clay mineral formation during podzolization in an alpine environment of the Tatra Mountains, Poland. *Clays and Clay Minerals*, **55**, 618–634.

Skiba, M. and Skiba S. (2005) Chemical and mineralogical index of podzolization of the granite regolith soils. *Polish Journal of Soil Science*, **38**, 153–162.

Skiba, M., Szczerba, M., Skiba, S., Bish, D.L., and Grybos, M. (2011) The nature of interlayering in clays fom a podzol (spodosol) from the Tatra Mountains, Poland. *Geoderma*, **160**, 425–433.

Środoń, J. (1999) Use of clay minerals in reconstructing geological processes: recent advances and some perspective. *Clay Minerals*, **34**, 27–37.

Środoń, J. (2003) Mixed-layer clays. Pp. 447–450 in: *Encyclopedia of Sediments and Sedimentary Rocks* (G. Middleton, editor). Springer, Dordrecht, Germany.

Środoń, J. and Gaweł, A. (1988) Identyfikacja rentgenograficzna mieszanopakietowych krzemianów warstwowych. Pp. 290–307 in: *Metody Badań Minerałów i Skał* (A. Bolewski and W. Żabiński, editors). Wydawnictwa Geologiczne, Warsaw.

Whitehouse, U.G. and McCarter, R.S. (1956) Diagenetic modification of clay mineral types in artificial sea water. *Clays and Clay Minerals*, **5**, 81–119.

(*Received 13 February 2013; revised 23 July 2013; Ms. 742; AE: M. Kawano*)